10B.3 DIAGNOSING THE INTERCEPT PARAMETER FOR EXPONENTIAL RAINDROP SIZE DISTRIBUTION BASED ON VIDEO DISDROMETER OBSERVATIONS

Guifu Zhang[1], Ming Xue[1,2], Qing Cao[1], and Daniel Dawson[1,2]
[1]School of Meteorology and [2]Center for Analysis and Prediction of Storms
University of Oklahoma, Norman OK 73072

1. Introduction

Information about the drop size distribution (DSD) is essential for understanding precipitation physics, estimating rainfall, and improving microphysics parameterizations in numerical weather prediction (NWP) models (Steiner et al. 2004). The characteristics of rain DSDs are often associated with the types of storms (e.g., convective versus stratiform rain) and their stages of development (e.g., the developing versus decaying stage, Brandes et al. 2006). Strong convective rain usually contains both large and small drops and has a broad DSD while the decaying stage is often dominated by small drops. Stratiform rain usually contain[1]s relatively larger drops but has a low number concentration for a given rain rate (Zhang et al. 2006).

Rain DSDs are usually represented by distribution models such as the exponential distribution, gamma distribution, and lognormal distribution. A DSD model usually contains a few free parameters that should be easy to determine and the model should be capable of capturing the main physical processes and properties. The exponential distribution is the most commonly used DSD model that has some of these properties, and it is given by

$$N(D) = N_0 \exp(-\Lambda D) . \qquad (1)$$

It contains two free parameters, N_0 and Λ. A single-moment bulk microphysics model predicts one of the moments of the DSD which determines one of the two parameters. The intercept parameter N_0 is usually specified so that Λ is uniquely related to the water content, W, which is the 3rd moment of the DSD that is predicted. The Marshall−Palmer (M-P, Marshall and Palmer 1948) exponential DSD model with the N_0 value fixed at 8000 m^{-3} mm^{-1} = 8×10^6 m^{-4} is widely used for representing warm rain (Kessler 1969) as well as ice (e.g., Lin et al. 1983; Hong et al. 2004) microphysics.

However, disdrometer observations and numerical model simulations indicate that N_0 and number concentration (N_t) are not constant, but vary depending on precipitation type, rain intensity and stage of development. Sauvageot and Lacaux (1995) showed variations of both N_0 and Λ from impact disdrometer measurements. Recent observations by 2D Video Disdrometers (2DVD) suggest that rain DSDs are better represented by a constrained Gamma distribution (Zhang et al. 2001) that also contains two free parameters. In Zhang et al. (2006), the constrained Gamma model was further simplified to a single parameter model for bulk microphysical parameterization and the model produced more accurate precipitation system forecasts than the M-P model. Since the exponential distribution model is widely used, a diagnostic relation of N_0 as a function of W would improve rain estimation and microphysical parameterization that are based on such an improved model.

In this study, we derive a diagnostic N_0 relation from rain DSD data that were collected in Oklahoma using disdrometers. To minimize the error effects introduced in the fitting procedure, we formulate the problem with a relation between two DSD moments. A diagnostic relation is found from the relation between two middle moments. Section 2 describes methods of deriving the diagnostic relation and section 3 presents results of diagnosing N_0 from water content using 2DVD measurements. In Section 4, we discuss applications of the diagnostic relation in the parameterization of rain physics and microphysical processes. Final summary and discussions are given in section 5.

2. Diagnosing methods

The diagnostic relation for the intercept parameter N_0 as a function of water content can be derived using two different approaches.

One approach is to first find the DSD parameters (N_0, Λ) by fitting DSD (e.g., disdrometer) data to the exponential function (1) for each DSD, and then plot the estimated N_0 versus W for the whole dataset for fitting a mean relation.

The n[th] moment of the exponential DSD (1) is

$$M_n = \int D^n N(D) dD = N_0 \Lambda^{-(n+1)} \Gamma(n+1) \quad . \qquad (2)$$

Hence, the DSD parameters, N_0 and Λ, can be determined from any two moments (M_l, M_m) as

[1]Corresponding author: Dr. Guifu Zhang
School of Meteorology, University of Oklahoma,
120 David L. Boren Blvd, Suite 5900, Norman OK 73072
E-mail: guzhang1@ou.edu

$$\Lambda = \left(\frac{M_l \Gamma(m+1)}{M_m \Gamma(l+1)} \right)^{\frac{1}{m-l}}, \quad (3)$$

$$N_0 = \frac{M_l \Lambda^{l+1}}{\Gamma(l+1)}. \quad (4)$$

When N_0 is obtained along with the water content W for DSD data sets, a $N_0 - W$ relation can be found through another fitting procedure, e.g., the power-law fitting. It is noted that the values of the estimated N_0 depend on which two moments are used and on the accuracy of the two moment estimates. Since the estimates of both the moments (M_l, M_m) have error, the DSD parameters (N_0, Λ) obtained from them will also have error. The natural variation in DSDs also causes a large scatter in the $N_0 - W$ plot (see Fig.1 in next section). Hence, the $N_0 - W$ relation derived from the above procedure tends to have larger errors.

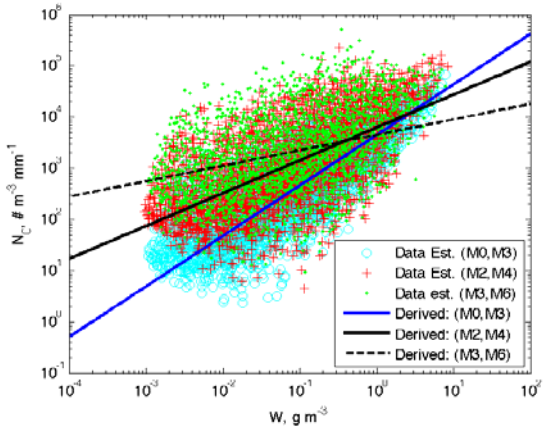

Fig. 1: Dependence of intercept parameter (N_0) on water content (W). Scattered points are fitted results from a pair of DSD moments. Straight lines are derived relations using the moment relation method.

To minimize the error effects introduced in the fitting procedures, we propose an alternative procedure for obtaining the $N_0 - W$ relation. Here, we first seek to establish a relation between two DSD moments. With this relation, the exponential distribution is reduced to having a single free parameter so that N_0 can be determined from W. Suppose that two DSD moments M_l, and M_m are related by a power-law relation:

$$M_l = a M_m^b, \quad (5)$$

where a and b are coefficients that can be estimated from disdrometer observations.

From Eq. (2) for the third moment, we have water content $W = \frac{\pi}{6} \rho M_3 = \pi \rho N_0 \Lambda^{-4}$, [$\rho$ is water density], yielding the slope parameter $\Lambda = \left(\frac{N_0 \pi \rho}{W} \right)^{1/4}$. Substituting (2) into (5) for M_l and M_m, and making use of the relation for Λ, we obtain

$$N_0 = \alpha W^{\beta}, \quad (6)$$

where

$$\alpha = \left(a \frac{\Gamma^b(m+1)}{\Gamma(l+1)\pi^c \rho^c} \right)^{\frac{1}{1-b+c}}, \quad (7)$$

$$\beta = \frac{c}{1-b+c}, \quad (8)$$

and

$$c = \frac{b(m+1) - (l+1)}{4}. \quad (9)$$

Hence, (6) - (9) constitute a general formulation for deriving a $N_0 - W$ relation using a statistical relation between two DSD moments. When the coefficients a and b in the relation (5) are determined from a set of DSD data, we have a diagnostic relation between the water content W and the intercept parameter N_0. This is the procedure that will be used in the next section with a disdrometer data set.

3. Derivation of the N_0–W relation from disdrometer observations

We test our method for deriving the $N_0 - W$ relation using disdrometer data collected in Oklahoma during the summer seasons of 2005 and 2006 (Cao et al. 2007). Three 2DVDs, operated respectively by the University of Oklahoma (OU), National Center for Atmospheric Research (NCAR) and National Severe Storms Laboratory (NSSL) were deployed at the NSSL site in Norman, Oklahoma, and at the Southern Great Plains (SGP) site of the Atmospheric Radiation Measurement (ARM) program. The ARM site is located approximately 28 km south of the NSSL site. A total of 58 days of disdrometer data covering a total of 13379 minutes of rainfall periods with total drop counts greater than 10 were collected. Among them are 1092 minutes of data that have side-by-side measurements by two 2DVDs. The recorded raindrops within each minute were processed to produce one-minute DSD samples, yielding a total of 13379 DSDs.

With the side-by-side data, measurement errors of DSDs were quantified. The sampling errors are further reduced by sorting and averaging based on two parameters (SATP), a method that combines DSDs with similar rainfall rates (R) and median volume diameters (D_0) (Cao et al. 2007). There are 1092 quality-controlled DSDs after SATP processing for the dataset. The DSD moments are estimated by the sum of weighted DSDs as defined in (2). Cao et al. (2007) showed that the middle

moments (M_2, M_3 and M_4) have the least error (see their Table 1).

The exponential DSD parameters N_0 and Λ are estimated from the moment pairs of (M_0, M_3), (M_2, M_4), and (M_3, M_6) using Eqs. (3) and (4). The exponentially-fitted N_0 values are plotted versus the rain water content in Fig. 1. As expected, there is a large scatter in the $N_0 - W$ plot because of measurement and model errors as well as natural variations. Also, different moment pairs produce different results of N_0 due to differences in estimation error and error propagation in the fitting procedure. It is clear that there is a positive correlation between N_0 and W. However, there will be high uncertainty if we were to fit the data points of this plot directly to a $N_0 - W$ relation.

Instead, an $N_0 - W$ relation is derived from a moment relation as outlined in section 2. Figure 2 shows the scatter plots of moment estimates for the pair of (M_2, M_4), and a power-law relation is obtained as

$$M_2 = 1.42 M_4^{0.836}, \qquad (10)$$

i.e., a = 1.42 and b = 0.836 in Eq.(5). The correlation between the moments is high, with a correlation coefficient of 0.88 in the linear domain and 0.93 in the logarithmic domain. Substituting for a and b in (6)-(9), we obtain α = 6257 and β = 0.642, therefore

$$N_0(M_2, M_4) = 6257 W^{0.642}. \qquad (11)$$

This N_0 - W relation is shown in Fig. 1 along with those derived from moment pairs (M_0, M_3) and (M_3, M_6). The lower (higher) moment pair yields a relation with a larger (smaller) power. As discussed earlier, the middle moment pair (M_2, M_4) has smaller error and therefore relation (11) is recommended.

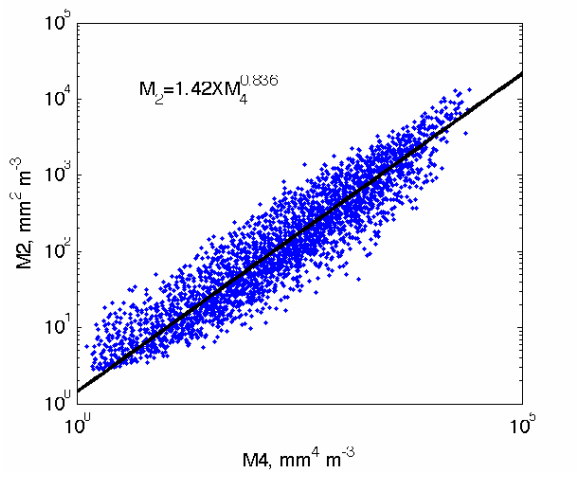

Fig. 2: Inter-relationships among DSD moments based on disdrometer measurements. Scattered points are direct estimates from disdrometer measurements. Straight lines represent fitted power-law relations.

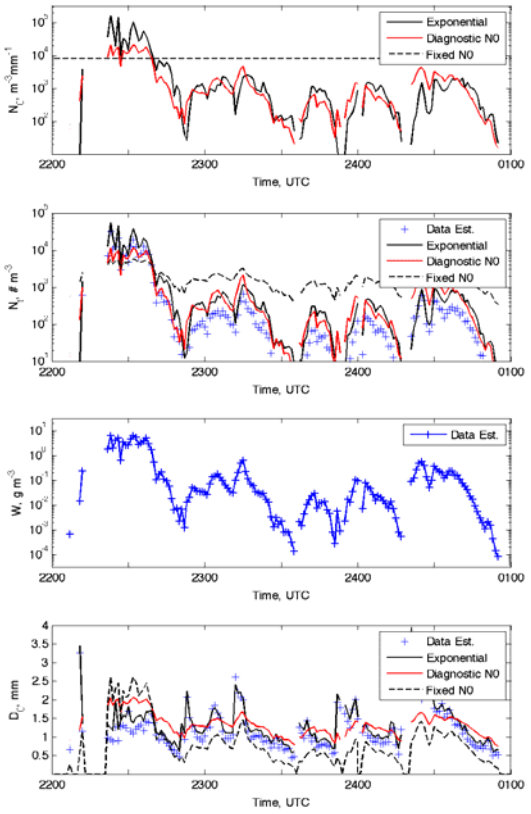

Fig. 3: Time series comparison of physical parameters: intercept parameter (N_0), total number concentration (N_t) water content (W), and median volume diameter (D_0) for a rain event starting on July 21, 2006. Results are shown for disdrometer measurements and fitted values using exponential, diagnostic-N_0, and fixed-N_0 DSD models.

For a better understanding of the $N_0 - W$ relation (11), Figure 3 shows an example of N_0 values along with other physical parameters (N_t, W, and D_0) as a function of time for a rain event starting on July 21, 2006. It was a strong convective storm followed by stratiform rain as well as weak convection passing over the OU disdrometer deployed at the ARM site at Washington, Oklahoma. The water content is very low during the stratiform precipitation period, but the median volume diameter D_0 is comparable to that of strong convection. The comparison between exponentially-fitted N_0 values from DSD moments M_2 and M_4 and those diagnosed from W using (11) is plotted in Fig. 3a. As shown in Fig. 3b, the moment fitting of the exponential DSD model yields a good estimate of total number concentration N_t as compared with the direct estimates from DSD data (discrete "+"). Here, the fitted N_0 can be considered as "truth" because N_0 is a model parameter which is obtained through the fitting procedure of Eqs. (2) - (4). It is clear that the diagnosed N_0 captures the main trend of the observed rain storm very well in a dynamic range

of more than two orders of magnitude; that is, from an order of 10^4 for strong convention to 10 for light stratiform precipitation. In comparison, the fixed-N_0 M-P model overestimates N_0 except for heavy convective rain. Figure 3d compares median volume diameter D_0 calculated from the DSD data, estimated using the diagnostic-N_0 model and that with the fixed-N_0 model. Again, the diagnostic $N_0 - W$ relation produces a much better agreement with the measurements than does the fixed-N_0 model.

4. Application to warm rain microphysical parameterization

The warm rain microphysical processes related to the DSD include rain evaporation, accretion of cloud water by rain water, and rain sedimentation. The microphysical parameters of these processes based on the exponential DSD model have been derived by Kessler (1969: Table 4). After unit conversion, the evaporation rate (R_e in kg kg^{-1} s^{-1}), accretion rate (R_c in kg kg^{-1} s^{-1}), mass-weighted terminal velocity (V_{tm} in m s^{-1}), and reflectivity factor (Z in mm^6 m^{-3}) are obtained as

$$\mathrm{R_e} = 2.17\times10^{-5} E_e N_0^{7/20} (q_{vs} - q_v) \mathrm{W}^{13/20}, \quad (12a)$$

$$\mathrm{R_c} = 1.65\times10^{-3} E_c N_0^{1/8} q_c \mathrm{W}^{7/8}, \quad (12b)$$

$$\mathrm{V_{tm}} = 16.4 N_0^{-1/8} W^{1/8} \left(\rho_0/\rho\right)^{0.5}, \quad (12c)$$

$$Z = 1.73\times10^{7} N_0^{-3/4} W^{7/4}. \quad (12d)$$

where E_e and E_c are the evaporation and accretion efficiency factors, respectively (normally taken as 1), W is rain water content in g m^{-3} as before ($W = 1000\rho q_r$), q_v, q_c and q_r are, respectively, the water vapor, cloud water and rain water mixing ratios in kg kg^{-1}.

Substituting the diagnostic relation (11) into (12) and assuming unit saturation deficit and unit cloud water mixing ratio as well as unit efficiency factors, we obtain a parameterization scheme based on the diagnostic N_0. The terms corresponding to those in Eq. (12) are listed in Table 1 along with those of the standard fixed-N_0 M-P model. The coefficients of these terms are similar for the two schemes, but the powers are substantially different. The larger power in evaporation rate means more (less) evaporation for heavy (light) rain compared to the fixed-N_0 model. The smaller power in the reflectivity formula for the diagnostic-N_0 model gives smaller (larger) reflectivity than the fixed N_0 for heavy (light) rain. This may lead to a better agreement between numerical model forecasts and radar observations. The former tends to over-predict large reflectivity values and under-predict low reflectivity values. In this sense, the diagnostic-N_0 model has similar properties as the simplified-constrained-gamma model investigated in Zhang et al. (2006)

Table 1: Parameterization of warm rain processes with diagnostic N_0 and fixed N_0

Parameterized quantity	Diagnostic N_0	Fixed N_0
N_0, m^{-3} mm^{-1}	$6257W^{0.642}$	8000
R_e, kg kg^{-1} s^{-1}	$4.63\times10^{-4}\mathrm{W}^{0.875}$	$5.03\times10^{-4}\mathrm{W}^{0.65}$
R_c, kg kg^{-1}s^{-1}	$4.92\mathrm{x}10^{-3}W^{0.955}$	$5.08\times10^{-3}W^{0.875}$
V_{tm}, m s^{-1}	$5.50W^{0.0447}$	$5.32W^{0.125}$
Z, mm^6 m^{-3}	$2.46\times10^{4}W^{1.27}$	$2.04\times10^{4}W^{1.75}$

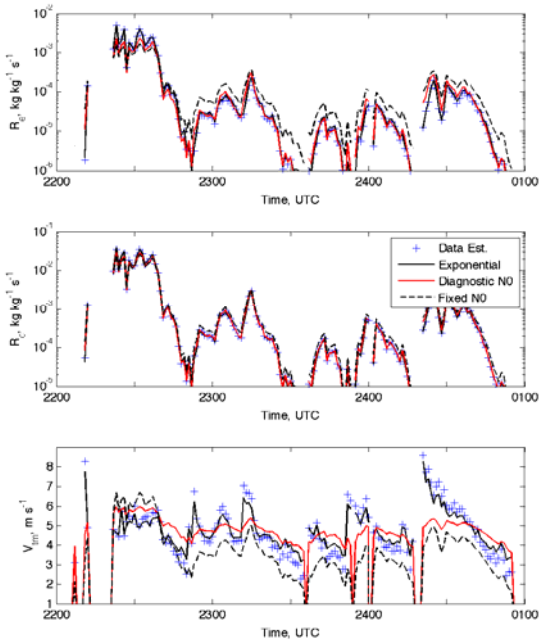

Fig. 4: As in Fig. 3 except for evaporation rate for a unit vapor saturation deficit (R_e), accretion rate (R_c) for a unit cloud water content, and mass-weighted terminal velocity (V_{tm})
DSD models.

Figure 4 compares the terms for the microphysical processes estimated from W using the diagnostic-N_0 DSD model with those from the fixed-N_0 M-P DSD model. Direct calculations from the observed DSD data and those fitted with the exponential model with N_0 as one of the two free parameters are also shown for reference. The results may appear to be close to each other in the semi-logarithm plots but actually, the fixed-N_0 model overestimates the evaporation rate for stratiform rain by about a factor of five and underestimates that for strong convection. This might be the reason that the parameterization coefficients in the Kessler scheme are sometimes reduced by a half and more in order to obtain

a better match of modeling results with observations (e.g., Sun and Crook 1997). The diagnostic-N_0 model therefore characterizes rain evaporation, accretion and rainfall processes more accurately than the fixed-N_0 model for both heavy and light rainfall. This is because by introducing the dependency of N_0 on W based on observations, raindrop number concentration and total surface area of rain drops are better represented, leading to a better estimation of evaporation and accretion rates.

5. Summary and Discussions

In this paper, we present a way of diagnosing the intercept parameter N_0 of the exponential distribution and apply the diagnostic-N_0 DSD model to improving warm rain microphysical parameterization. The diagnostic relation is derived from a relation between two DSD moments that are estimated from 2D video distrometer data. The DSD data were collected in Oklahoma during the summer seasons of 2005 and 2006, which should be representative for rains in the central Great Plains region. The $N_0 - W$ relation is used to improve the Kessler parameterization scheme of warm rain microphysics, and can be used in schemes containing ice-phases also (e.g., Lin et al. 1983; Hong et al. 2004).

It has been shown that the diagnostic-N_0 model better characterizes natural rain DSDs, including the physical properties (e.g., N_t, and D_0) and microphysical processes. For a given water content, the diagnostic-N_0 DSD model represents the total number concentration, median volume diameter, reflectivity factor, evaporation rate and accretion rate much more accurately than the M – P model with a fixed N_0. Compared with the M-P model-based Kessler scheme, the modified parameterization scheme with a diagnostic N_0 has the following advantages: (i) it leads to less (more) evaporation for light (heavy) rain and therefore can preserve stratiform rain better in numerical models, and (ii) it yields a larger (smaller) reflectivity factor for light (heavy) rain, having the potential of yielding a better agreement between model predicted and radar observed reflectivities in a similar way as the simplified constrained gamma model. Realistic simulation of reflectivity is important for assimilating radar reflectivity data into NWP models.

It is noted that the diagnostic $N_0 - W$ relation obtained in this paper is based on a specific set of disdrometer data in the summer season of a specific climate region. While the methodology developed in this paper is general, the coefficients in the relation may need to be tuned to better fit specific regions and/or seasons or specific rain types. The improved parameterization based on the diagnostic-N_0 model is now being tested within the Advanced Regional Prediction System (ARPS, Xue et al. 2003) to examine its impact on precipitation forecast; the results will be presented in a future paper.

Acknowledgments Authors greatly appreciate helps from Drs. Edward Brandes, Terry Schuur, Robert Palmer, Phillip Chilson and Ms. Kyoko Iketa. The sites for disdrometer deployment at the Kessler farm were provided by Atmospheric Radiation Measurement (ARM) Program. This work was primarily supported by a NSF grant ATM-0608168. Dan Dawson were also supported by NSF grants ATM-0530814 and Ming Xue further by ATM-0331594 and ATM-0331756.

References

Brandes, E. A., G. Zhang, and J. Sun, 2006: On the influence of assumed drop size distribution form on radar-retrieved thunderstorm microphysics. *J. Appl. Meteor*, 45, 259-268,

Cao, Q., G. Zhang, E. Brandes, T. Schuur, A. Ryzhkov, and K. Ikeda, 2007: Analysis of video disdrometer and polarimetric radar data to characterize rain microphysics in Oklahoma. *J. Appl. Meteor. Climat. Under review.*

Hong, S.-Y., J. Dudhia, and S.-H. Chen, 2004: A revised approach to ice microphysical processes for the bulk parameterization of clouds and precipitation. *Mon. Wea. Rev.,* **132,** 103–120.

Kessler, E., 1969: On the distribution and continuity of water substance in atmospheric circulations. *Meteor. Monogr.,* No. 32, Amer. Meteor. Soc., 84 pp.

Lin, Y.-L., R. D. Farley, and H. D. Orville, 1983: Bulk parameterization of the snow field in a cloud model. *J. Climate Appl. Meteor.,* **22,** 1065−1092.

Marshall, J.S., and W. McK. Palmer, 1948: The distribution of raindrops with size, *J. Meteor*., **5**, 165-166.

Sauvageot, H., and J.-P. Lacaux, 1995: The shape of averaged drop size distributions. *J. Atmos. Sci*., **52**, 1070–1083.

Steiner, M., J. A. Smith, and R. Uijlenhoet, 2004: A microphysical interpretation of radar reflectivity-rain rate relationships. *J. Atmos. Sci*., **61**, 1114-1131.

Sun, J, and N. A. Crook, 1997: Dynamical and microphysical retrieval from Doppler radar observations using a cloud model and its adjoint. Part I: Model development and simulated data experiments. *J. Atmos. Sci*., **54**, 1642–1661.

Xue, M., D.-H. Wang, J.-D. Gao, K. Brewster, and K. K. Droegemeier, 2003: The Advanced Regional Prediction System (ARPS), storm-scale numerical weather prediction and data assimilation. *Meteor. Atmos. Physics*, **82**, 139-170.

Zhang, G., J. Vivekanandan, and E. Brandes, 2001: A method for estimating rain rate and drop size distribution from polarimetric radar measurements. *IEEE Trans. Geosci. Remote Sens.,* **39,** 830–841.

Zhang, G., J. Sun, and E. A. Brandes, 2006: Improving parameterization of rain microphysics with disdrometer and radar observations. *J. Atmos. Sci.,* **63**, 1273-1290 .